DEVELOPMENT OF TEXAS-V CODE SURROGATE MODEL FOR ASSESSMENT OF STEAM EXPLOSION IMPACT IN NORDIC BWR

D. Grishchenko, S. Basso, S. Galushin and P. Kudinov*

Division of Nuclear Power Safety, Royal Institute of Technology
Roslagstullsbacken 21, SE-106 91, Stockholm, Sweden
dmitry@safety.sci.kth.se, simoneb@kth.se, pavel@safety.sci.kth.se

ABSTRACT

Severe accident mitigation strategies in Nordic boiling water reactors (BWRs) employ core melt cooling in a deep pool of water under the reactor pressure vessel. Corium melt released from the vessel is expected to fragment, solidify and form a porous debris bed coolable by natural circulation. However, steam explosion can occur upon melt release threatening containment integrity and potentially leading to large early release of radioactive products to the environment. Significant aleatory and epistemic uncertainties exist in accident scenarios, melt release conditions, and modeling of steam explosion phenomena. Assessment of the risk of ex-vessel steam explosion requires application of the Integrated Deterministic Probabilistic Safety Analysis (IDPSA). IDPSA is a computationally demanding task which makes unfeasible direct application of Fuel-Coolant Interaction codes.

The goal of the current work is to develop a Surrogate Model (SM) of the TEXAS-V code and demonstrate its application to the analysis of explosion impact in the Nordic BWR. The SM should be computationally affordable for IDPSA analysis. We focus on prediction of the steam explosion loads in a reference Nordic BWR design assuming a scenario of coherent corium jet release into a deep water pool. We start with the review of the TEXAS-V sub-models in order to identify a list of parameters to be considered in implementation of the SM. We demonstrate that TEXAS-V exhibits chaotic response in terms of the explosion impulse as a function of the triggering time and introduce a statistical representation of the explosion impulse for given melt release conditions and arbitrary triggering time. We demonstrate that characteristics of the distribution are well-posed. We then separate out the essential portion of modelling uncertainty by identification of the most influential uncertain parameters using sensitivity analysis. Both aleatory uncertainty in characteristics of melt release scenarios and water pool conditions, and epistemic uncertainty in FCI modeling are considered. Ranges of the uncertain parameters are selected based on the available information about prototypic severe accident conditions in a Nordic BWR. A database of TEXAS-V solutions is generated and used for the development of the SM. Performance, predictive capability and application of the SM to risk analysis are discussed in detail.

KEYWORDS
Severe accident, ex-vessel steam explosion, sensitivity study, surrogate model, IDPSA, ROAAM+

---

* Corresponding author

1. INTRODUCTION

The goal of this work is to establish a comprehensive approach to the analysis of the ex-vessel steam explosion in a Nordic BWR using the TEXAS-V code. The key aspect of the methodology is that it does not follow the best estimate or conservative practices but is based on statistical assessment of the confidence levels for explosion impulse. It should be noted that complete risk analysis would imply definition of melt release conditions with appropriate probability density functions and therefore modelling of the severe accident progression starting from reactor failure. Such modelling is beyond the scope of the article. Instead we define the ranges of melt release conditions that we consider relevant for the Nordic BWR; within these ranges we develop a map of explosion impulses, and then construct the failure domain by comparison of the loads and specific to Nordic BWR containment fragilities.

In the first part of the paper we (i) provide review of TEXAS-V, (ii) report implementation of the TEXAS-V model for assessment of the steam explosion in a Nordic BWR along with simplified impulse propagation method, and (iii) estimate the distributions of the explosion impulse at the center of the containment base. We discuss important findings of the modelling which are built upon the demonstrated physical ill-posedness of the code and stochastic nature of the steam explosion phenomena.

In the second part, we start with the brief definition of the methodology used for failure domain identification and elaborate on our approach to the assessment of the steam explosion load given the inherent chaotic nature of steam explosion calculations. We demonstrate the necessity and results of surrogate model development and sensitivity study. We finish with the demonstration of failure domains and provide summary of the results and outlook in the Conclusions.

2. APPLICATION OF TEXAS-V FOR THE MODELLING OF PREMIXING AND STEAM EXPLOSION IN NORDIC BWR

2.1. Review of TEXAS-V

Texas-V is a 1D 3-field transient code with Eulerian fields for gas and liquid and a Lagrangian field for fuel particles. It is comprised of two modules for calculation of: premixing and steam explosion.

The premixing model is based on (i) two constitutive relations: the *fragmentation model for mixing* and the *phase change model;* (ii) two alternative modes of melt release: in the form of a coherent jet and in the form of discreet master particles; and (iii) two alternative mechanistic approaches for jet front breakup: *leading edge* and *trailing edge*.

The *fragmentation model for mixing* is comprised of three mechanisms: Kelvin-Helmholtz instability, boundary layer stripping and Rayleigh-Taylor instability. The former two are considered to have minor effect with vapor film present and are reduced rapidly with rise of void fraction. The model considers the fuel particles to be deformed and dynamically fragmented into a discrete number of particles from its initial diameter to smaller size (see Chu [1]):

$$D_f^{n+1} = D_f^n \cdot \left[1 - C_0 \Delta T^+ \cdot \left(\frac{\rho_c U_{rel}^2 D_f^n}{\sigma_f}\right)^{0.25}\right]$$

$$\Delta T^+ = \frac{U_{rel} \cdot (t^{n+1} - t^n)}{D_f^n} \cdot \left(\frac{\rho_c}{\rho_f}\right)^{0.5}$$

$$C_0 = 0.1093 - 0.0785 \cdot \left(\rho_c/\rho_f\right)^{0.5}$$

where n is time iteration index; D_f is fuel particle diameter; ΔT^+ is dimensionless time step; U_{rel} is relative velocity; t is time; σ_f is fuel surface tension; ρ_f, ρ_c are densities of fuel and coolant respectively.

Therefore, the primary breakup is dominated by the existence of the jet front, the moment the jet front reaches the bottom of the domain primary breakup sharply reduces. It is further assumed that coherent fuel jet will not breakup until the fuel particle at the leading edge, exposed to the oncoming coolant, is fragmented (and swept away from the interface), that is only a master particle at the leading edge of the jet can be subject to fragmentation.

The onset of master particle fragmentation is driven by one of the mechanistic approaches for jet front breakup. *The trailing edge* algorithm forces a leading master particle to fragment at the tail of the fragmented debris, i.e. at the beginning of the premixing region. The *Leading edge* algorithm implies the start of the leading master particle fragmentation at the leading front of the fragmented debris, i.e. at the end of the premixing region. The trailing edge regime provides very slow jet propagation compared to the trailing edge approach and consequently longer time for primary breakup and higher steam generation rates. Supposedly, it is intended to predict fragmentation and propagation of small jets prone to sinusoidal instability. Given characteristic scales of melt release in the reactor case and comparing jet front propagation velocity in water with that predicted by MC3D we have found the leading edge algorithm to provide more adequate prediction of jet propagation velocity (as opposed to trailing edge algorithm).

The phase change model (in continuous liquid field) is comprised of two primary equations that define:
1. Heat loss from fuel particles $\dot{q}_{fuel}$:

$$-\dot{q}_{fuel} = \pi D_f^2 h_{film}\left(T_f - T_{sat}\right) + \pi D_f^2 \sigma F\left(T_f^4 - T_{sat}^4\right),$$

where the first term on r.h.s. describes convection heat transfer rate from the fuel particle to the liquid vapor interface, and the second term is the radiation heat transfer rate from the fuel particle to the saturated liquid-vapor interface. The temperature profile inside a particle is solved in a simplified way using a steady state approach: it is assumed spatially constant in the bulk and linearly decreasing within a thin thermal layer δ.

The corresponding steam generation rate $\dot{M}_{s,p}$ is than derived from:

$$-\dot{q}_{fuel} = \pi\left(D_f + 2\delta_{film}\right)^2 h_{lg}\left(T_f - T_{sat}\right) + C_{rad}\pi D_f^2 \sigma F\left(T_f^4 - T_{sat}^4\right) + \dot{M}_{s,p}h_{fg},$$

where the first term on the r.h.s. is convection heat transfer rate from the liquid-vapor interface around the fuel particle to bulk liquid field and the second term is the fraction C_{rad} of radiation heat flux that is absorbed in the subcooled liquid; h_{fg} is the latent heat of steam.
2. Heat flux balance around steam bubbles and resulting steam generation rate $\dot{M}_{s,b}$:

$$A_{gL}K_g \frac{\left(T_g - T_{sat}\right)}{\delta_g} = A_{gL}h_{L.sL}\left(T_{sat} - T_L\right) + \dot{M}_{s,b}h_{fg}$$

where the term on the l.h.s. is the vapor bubble-side heat transfer rate; the first term on the r.h.s. is the bulk liquid-side heat transfer rate; A_{gL} is the surface area of the interface between the liquid field and the vapor field as determined from the vapor bubble radius and the flow regime; K_g is effective thermal conductivity of the vapor film.

The net rate of steam generation $\dot{m}_s$ per unit volume is thus expressed in terms of the net heat flux $\dot{q}_{net,f}$

$$\dot{m}_s = \frac{\dot{q}_{net,f}}{h_{fg}V_{cell}} \tag{1}$$
$$\dot{q}_{net,f} = \dot{q}_{fuel} - \dot{q}_l - \dot{q}_v$$

where $\dot{q}_l$ and $\dot{q}_v$ are the heat received by coolant liquid and coolant vapor respectively, which becomes the internal energy of the coolant; and V_{cell} is cell volume.

The **fine fuel fragmentation** (upon steam explosion) is due to the fragmentation model proposed by Tang and Corradini [3, 4] which is largely based on the original Kim's model [2]. It is a combination of thermal and hydrodynamic effects. Being computationally expensive it is replaced in TEXAS with a semi-empirical equation where fine fragmentation rate $\dot{m}_f$ is expressed as:

$$\dot{m}_f = C m_p \cdot \left(\frac{P - P_{th}}{\rho_c R_p^2} \right)^{0.5} F(\alpha) g(\tau) \tag{2}$$

where m_p is mass of the initial particle; R_p is radius of the initial particle; P_{th} is the threshold pressure necessary to cause film collapse; P is ambient pressure; $F(\alpha)$ is the compensation factor for coolant void fraction ($F(\alpha)$ decreases from 1 to 0 at void fraction $\alpha = 0.5$); and $g(\tau)$ is the factor for available fragmentation time.

The threshold pressure P_{th} is evaluated based on theoretical work by Kim and experimental data. At ambient pressure 1 Bar the threshold pressure is in the range from 2 to 4 Bars. As the ambient pressure increases the threshold pressure also increases, however no definite quantitative values have been suggested.

The integral fragmentation mass depends on the duration of the fragmentation process. The factor $g(\tau)$ is introduced as an empirical approach to account for the characteristic fragmentation time τ during which the above mechanism is considered to be operative. The factor $g(\tau)$ decreases from 1 to 0 as this characteristic time is exceeded. At ambient pressure (1Bar) the recommended value for it is 1-4 ms. It is indicated that as ambient pressure increases the fragmentation limit time decreases.

The heat generated due to dynamic fine fragmentation is expressed in TEXAS as:

$$\dot{q}_{frag} = \dot{m}_f \cdot \left(C_{pf} \cdot \left(T_f - T_s \right) + i_f \right) \tag{3}$$

where i_f is fuel latent heat; T_f is fuel temperature; T_s is saturation temperature of the coolant; C_{pf} is specific heat for the fuel. Due to extremely fine fragmentation of the fuel the rate of heat transfer is so fast that it is assumed to generate steam only giving the following equation for steam generation rate $\dot{m}_s$ per unit volume:

$$\dot{m}_s = \frac{\dot{q}_{net,f} + \dot{q}_{frag}}{h_{fg}V_{cell}} \tag{4}$$

Further details on the implemented models in TEXAS can be found in the thesis by Chu [1] for premixing model and by Tang [3] for propagation model or in the TEXAS-V manual [4].

2.2. Model implementation

Modelling of steam explosion was implemented assuming release of a single melt jet. In the calculations the jet diameter was varied in the range between 70 to 300 mm; initial system pressure between 1 and 4 bars; water subcooling in the range from 10 to 128 K, water pool depth between 5 and 9 m. The height of the computational domain, from the point of melt release to the bottom of the water pool, was 13.0 m.

The computational domain was vertically divided onto 26 cells, each 0.5 m high with the same cross section area. The effect of the cell height on TEXAS-V calculations was separately studied. Results suggest that with the decrease of the cell height in the range from 0.2 to 0.4 m explosion impulses get weaker and the number of failed calculations increases; explosion impulses were not affected when mesh cell height was varied from 0.4 to 0.6 m.

The mesh cell cross section area has profound effect on the dynamic pressure and consequently on the explosion pressure impulse. A robust approach to defining the cell cross section area would require application of a 2D FCI code to determine the minimal radial extent of the premixing region where averaged 2D solution remains independent from the radial extent. This is a tedious and complex task. However, it was found that in TEXAS-V for the chosen ranges of input parameters the product of the pressure impulse and cell cross section area [m^2] is practically independent from the cell cross-section area (see **Figure 1**). Considering further that TEXAS-V was extensively validated against KROTOS experimental data, we set the ratio of the jet radius (R_{jet}) to cell radius (R_{cell}) approximately the same as in the KROTOS experiments. In this work the following relation has been used:

$$R_{cell} = 11.0 \cdot R_{jet} \qquad (5)$$

Reduced time steps were chosen to decrease the number of failed calculations, specifically, the time step for premixing calculations was set from 10^{-8} to 10^{-6} s and the time step for explosion was in the range between 10^{-8} and $5 \cdot 10^{-7}$ s.

All computational results reported hereafter were obtained using the leading edge breakup mechanism and coherent jet release model. The model for hydrogen generation [5] was not used.

Two response functions were derived from the TEXAS-V calculations: one for the characterization of the steam explosion, i.e. explosion impulse (F_{expl}); and one for the characterization of the premixing, i.e. total surface area of liquid melt droplets in water (F_{prmx}).
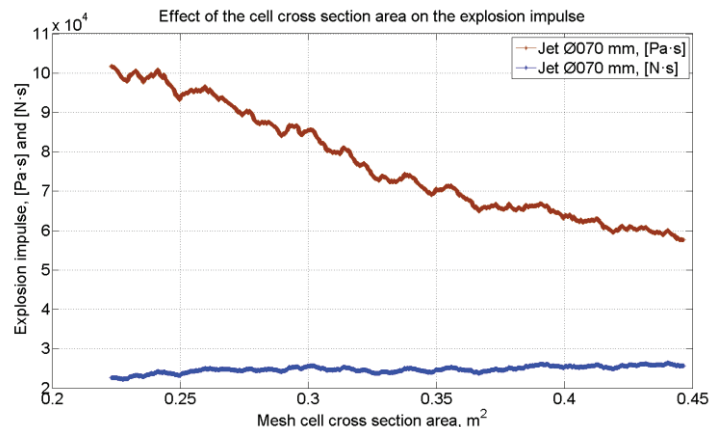

Figure 1: Effect of the mesh cell cross section area on the explosion impulse

Explosion impulse was integrated from the dynamic pressure history:

$$F_{expl} = \max\left(\sum_i (P_{ij} - P_{0j})\delta t_i\right) \cdot A_{cell}, \ [N \cdot s] \tag{6}$$

where P_{ij} is pressure in the cell j at the time instance i; P_{0j} is pressure in the cell j at time 0; δt_i is the time step at the time instance i, A_{cell} – mesh cell cross section area.

The total surface area of liquid melt droplets in water was approximated as:

$$F_{prmx} \propto \sum_k \begin{cases} n_k R_k^2, & [Vs_{i(k)} < 0.5, \ T_k > T_{melt}] \\ 0, & otherwise \end{cases}, \ [m^2] \tag{7}$$

where k is Lagrangian particle group number; R_k is particle radius in the k particle group; n_k is number of particles in k particle group; T_k is particle bulk temperature in the k particle group; T_{melt} is melting temperature of the fuel; $Vs_{i(k)}$ is steam fraction in the cell i where k particle group is located.

The explosion impulse in eq. (6) is in [N·s]. In order to make it meaningful for risk analysis one must refer it to a specific area (provide explosion pressure impulse [Pa·s]), and apply an appropriate impulse propagation method to estimate the explosion impulse at relevant locations in the containment.

For demonstration purposes it is assumed that the explosion pressure impulse I [Pa·s] (similar to pressure distribution in a propagating spherical shock wave) is a decaying function of distance r from the center of the explosion:

$$I = \tilde{c} \cdot r^\nu, \nu \cong -1, \tilde{c} = const \tag{8}$$

The constant $\tilde{c}$ in eq.(8) can be estimated assuming explosion impulse F_{expl} to be distributed over the complete area of the containment base A_b and considering the point source of the explosion to be located in the center of the corresponding cell in TEXAS:

$$I_b = F_{expl}/A_b \tag{9}$$

$$I_b = \frac{2}{r_b^2} \int_0^{r_b} \frac{\tilde{c}}{(h_c^2 + r^2)^{0.5}} \cdot r dr \tag{10}$$

$$I(r) = I_b \cdot \frac{r_b^2}{2 \cdot ((r_b^2 + h_c^2)^{0.5} - h_c)} \cdot \frac{1}{r} \tag{11}$$

where r_b is the radius of the containment; h_c is elevation of the computational cell above the bottom of the domain. The impulse $\bar{I}_0$ at the center of the containment floor, i.e. at $r = h_c$, is then:

$$\bar{I}_0 = I_b \cdot \frac{r_b^2}{((r_b^2 + h_c^2)^{0.5} - h_c)} \cdot \frac{1}{2 \cdot h_c} \tag{12}$$

2.3. Results and Discussions

The time dependences of normalized premixing and explosion response functions are provided in **Figure 2**. The data was obtained given fixed melt release conditions. The first ~1.4s of melt release correspond to the jet propagation above the water pool. The following ~300 ms of melt-water interaction occur with no apparent correlation between the two functions. Then the two response functions develop correlated and periodic behavior. The latter is most likely driven by the periodic arrival of jet particles and the competing nature of the secondary fragmentation rate and rate of fine particles solidification. Note that if the premixing response function was defined as liquid melt volume / mass, i.e. taken proportional to $\sum n_k R_k^3$ the corresponding curve in **Figure 2** would be monotonously rising.

Figure 2 demonstrates that small variations in the triggering time lead to large changes in the explosion energetics. For example, between 1.90 and 2.01 s, i.e. within 110 ms time window, the explosion impulse changes almost 50 times, i.e. from 377 kPa·s to 8 kPa·s.

High sensitivity of the explosion impulse to the triggering time has far-reaching consequences which are not necessarily TEXAS specific. First, it demonstrates physical ill-posedness of FCI codes, i.e. chaotic nature of the steam explosion impulse with respect to the discreet triggering time. If triggering time is not properly treated, interpretation of FCI code results and code parametric studies becomes a subject of considerable uncertainty. It is instructive to note that among previous parametric studies, validation and evaluation of the TEXAS code [6, 7, 8] none have mentioned or addressed ill-posedness. This is not surprising given the rather limited (on the order of 10) number of supporting TEXAS computations.
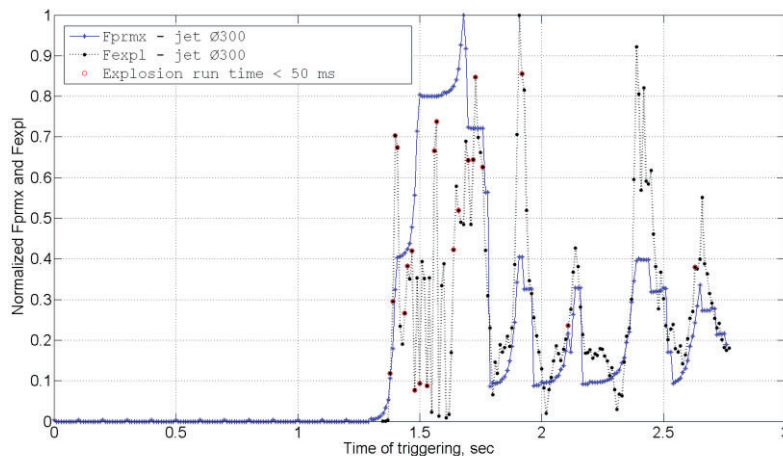

Figure 2: Dependence of premixing and explosion criterions on the triggering time (release of oxidic corium melt with jet Ø300 mm into a 7 m deep water pool)

Second, from the risk perspective, the choice of the triggering time given specific conditions of melt release can alter containment failure from physically unreasonable to physically unavoidable. In this sense choice of the triggering time should be driven by probabilistic or statistic considerations and should not be leveled by conservative or best estimate arguments.

Third, in FCI experiments the chaotic nature of steam explosion is expected to manifest in a stochastic way. The reason is the aleatory variability of the triggering time and melt release conditions that are not controlled or measured. Considering impulse ranges in **Figure 2**, the expected magnitude of the aleatory uncertainty in the experimental steam explosion impulses can potentially exceed the effect of other parameters controlled or intentionally varied in experiments.

In **Figure 3** we provide cumulative distributions of the explosion impulse calculated for reference Nordic BWR using TEXAS-V and propagated to the basement center according to the eq.(12). The data was obtained assuming uniform distributions for input parameters and running explosion calculations for every 4 ms of premixing time. The total number of computed explosion cases is 188251, number of different melt release conditions is 544, and number of varied parameters is 13.

According to the results demonstrated in **Figure 3** steam explosion impulse is a monotonic function of the inlet jet diameter: the explosion energetics increases with increase of the inlet jet diameter. Regardless of the range of jet diameter the explosion impulse covers the range with 3 orders of magnitude from 10^2 to 10^5 Pa·s. This again supports the idea that risk analysis of the containment failure due to steam explosion requires a robust approach involving statistical treatment of the aleatory uncertainty. Furthermore, choice of melt release conditions that should provide conservative assessment might be challenging: more than 86% of the total impulse range (from 50 kPa·s to 382 kPa·s) is established in less than 0.70% of cases (see insert in **Figure 3**).
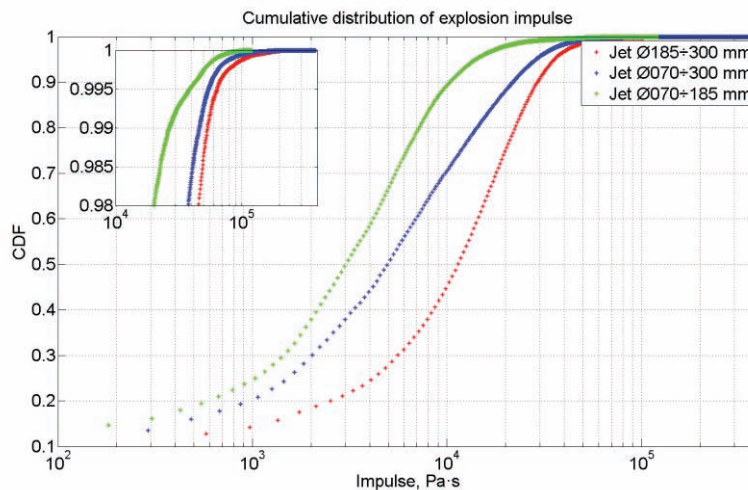
Figure 3: Distribution of impulse $\bar{I}_0$ predicted by TEXAS-V for different ranges of jet diameter.

3. APPLICATION OF TEXAS-V FOR THE IDENTIFICATION OF FAILURE DOMAIN DUE TO STEAM EXPLOSION IN A NORDIC BWR

3.1. Methodology

The TEXAS-V implementation of the Nordic BWR described in the previous chapter is used for data generation in the following development. We utilize the so called reverse analysis to build the domain of containment failure due to steam explosion. Reverse analysis is a part of ROAAM+ probabilistic framework developed in [9] and an extension of the classical ROAAM (Risk Oriented Accident Analysis Methodology) [10, 11].

In reverse analysis the space of scenario parameters (i.e. jet diameter, water pool depth, water pool temperature etc.) is partitioned into a finite number of cells. The output of TEXAS-V is sampled in each cell by varying model form (deterministic and intangible) parameters. The framework compares loads against capacity and renders every computed case to a failure or success. The number of "fail" and "success" cases is counted in each cell, weighted by corresponding probability density functions of model form parameters and normalized to provide conditional failure probability, which is then compared to a

screening threshold (0.001). The cells where conditional failure probability exceeds the screening threshold are grouped into the failure domain.

Reverse analysis is a computationally demanding task. Its application for steam explosion studies can be accomplished only if the framework for reverse analysis uses a fast counterpart of TEXAS-V, i.e. a Surrogate Model (SM).

A surrogate model [12] is a numerical tool that besides being a computationally efficient and numerically stable substitute of the parent code (Full Model) can allow processing / adaptation of the parent code output to the needs of a specific application. Development of an SM from the FM requires (i) definition of a well-posed response function to be predicted by the SM, (ii) identification of the FM most influential parameters to minimize the SM input space, (iii) generation of the sufficient database of FM solutions for (iv) the implementation and validation of the SM.

3.2. Definition of the well-posed response function

In the context of TEXAS-V, the response function is the steam explosion impulse. Previous results demonstrate that explosion impulse is ill-posed, i.e. exhibits chaotic behavior with respect to the triggering time. Aleatory variability of the explosion impulse can be encompassed by establishing its statistical characterization. For simplicity we estimate mean $\bar{F}_{expl}$ and standard deviation $\bar{F}_{std}$ of the explosion impulses obtained varying the triggering time:

$$\bar{F}_{expl} = \frac{1}{N} \sum_{m=1}^{N} F_{expl_m} \tag{13}$$

$$\bar{F}_{std} = \left[\frac{1}{N} \sum_{m=1}^{N} \left(F_{expl_m} - \bar{F}_{expl} \right)^2 \right]^{\frac{1}{2}} \tag{14}$$

where m is index for the discreet triggering time $t_{trig} = t_0 + dt_{trig} \cdot m$.

It can be demonstrated that the group $\{\bar{F}_{expl}, \bar{F}_{std}\}$ is well-posed and therefore can be used for SM development. Formulation of the response function as a combination of mean and standard deviation is beneficial as it allows interpretation of loads in terms of confidence intervals and confidence levels, for example $P(Impulse < \bar{F}_{expl} + 3 \cdot \bar{F}_{std}) = 0.999$.

Note that in general aleatory variability of the explosion impulse is not normally distributed and actual confidence levels are expected to be lower. We stick to this assumption only for demonstration purposes.

3.3. Sensitivity Study of TEXAS-V

Out of about 200 TEXAS-V input parameters 23 were selected for the analysis. The complete list is provided in **Table 1**. Note that indicated in **Table 1** ranges for sensitivity study were partially affected by TEXAS-V numerical stability; respective details are beyond the scope of this article.

Other parameters not mentioned in **Table 1** were set either in accord with the TEXAS-V manual [4] or according to recommendations in literature [6,7,8,16].

Table 1: List of TEXAS-V parameters used in the study

Parameter	Units	Range	Description
PO	**Pa**	**1-4 E05**	**Initial pressure**
TLO	**K**	**288-366**	**Water temperature**
XPW	**m**	**3.2-8.2**	**Water level in the containment**
TGO	K	TLO	Cover gas temperature
TWO	K	TLO	Wall temperature
RPARN	m	0.07	Fuel injection radius
		0.15	
CP	**J/kg·K**	**400-570**	**Fuel capacity**
RHOP	**kg/m3**	**7600-8600**	**Fuel density**
PHEAT	**J/kg**	**260-360 E03**	**Fuel latent heat**
TMELT	K	2850	Fuel melting temperature
TPIN	**K**	**2850-3150**	**Fuel injection temperature**
UPIN	**m/sec**	**1.5-2.5**	**Fuel injection velocity**
KFUEL	**W/m·K**	**2-11**	**Fuel thermal conductivity**
C(32)	**J/m2**	**0.4-0.6**	**Fuel surface tension**
C(18)	**-**	**0.6-0.9**	**Fuel emissivity**
DXI	m	0.5	Cell height
ARIY	**m²**	**0.7-1.8**	**Cell cross-section area**
		3.8-8	
TMAX	sec	-	Premixing time
CFR	**-**	**2.0-2.7 E-03**	**constant for rate of fuel fine fragmentation**
RFRAG	**m**	**8-1.2 E05**	**Initial size of fragmented particles**
POLD	Pa	2×PO	Threshold pressure for film collapse
TFRAGLIMT	**s**	**0.0005-0.0030**	**Fuel fragmentation time interval**
PTRIG	Pa	3E05	Trigger pressure

The sensitivity study was performed using the Morris method [13,14,15] and addressed 16 input parameters (listed in bold in **Table 1**). The mean explosion impulse ($\bar{F}_{expl} \cdot A_{cell}$, [Pa·s]) has been used as the response function. The results in **Figure 4** are provided for 140 mm jet diameter. The elements in the legend are sorted in descending order of the Morris μ value. The error bars demonstrate the spread of the results established in 3 consecutive sensitivity studies that used slightly different number of trajectories.
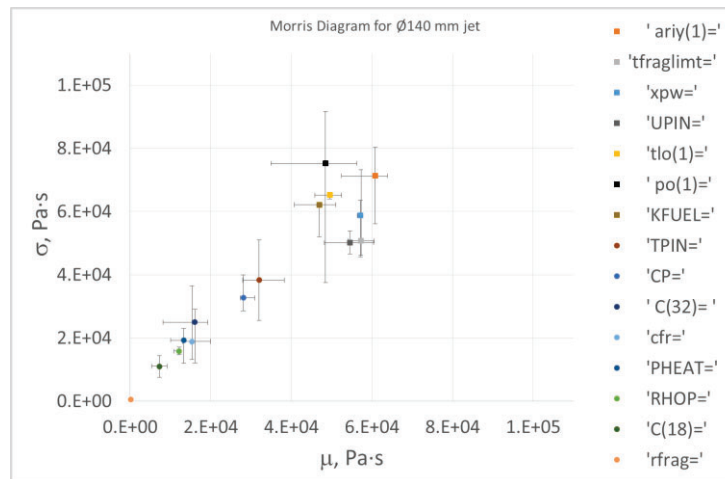

Figure 4: Morris diagrams for mean explosion impulse given fixed melt jet release diameter

Given rather high values of Morris σ we could justifiably screen out only three parameters: RFRAG, C(18) and ARIY (appearance of ARIY at the top of the list is artificial, recall results in **Figure 1**).

3.4. Surrogate Model Development

The surrogate model has been developed using Artificial Neural Networks (ANNs). The ANN is trained to predict the mean and standard deviation of the impulse $\bar{I}_0$ at the center of the containment floor given 13 TEXAS-V parameters in the input: XPW, PO, TLO, RPARN, CP, RHOP, PHEAT, TMELT, TPIN, UPIN, KFUEL, CFR, and TFRAGLIMT.

The parity plots provided in the **Figure 5** and **Figure 6** demonstrate satisfactory agreement between SM predictions and TEXAS-V calculations. Though, extension of the current database of TEXAS-V solutions is required to further improve the SM.
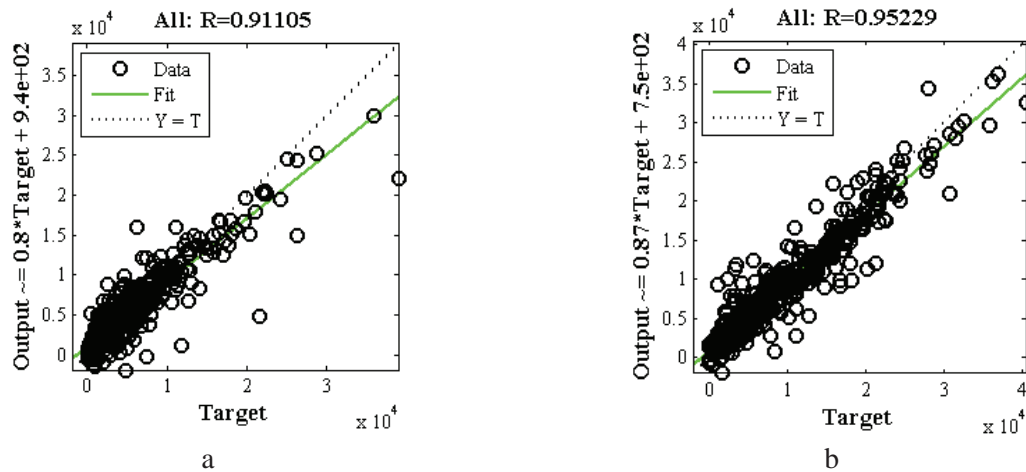
Figure 5: Parity plots of explosion mean (a) and standard deviation (b) for the training dataset
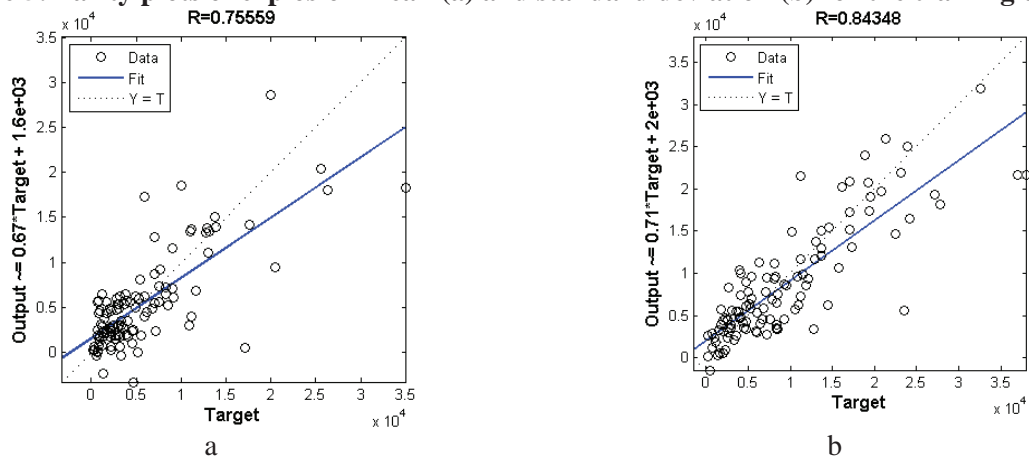

Figure 6: Parity plots of explosion mean (a) and standard deviation (b) for the testing dataset

3.5. Results and Discussions

The failure domains have been computed for three modes of melt release: Ø70, Ø150 and Ø300 mm jets; two types of distributions for deterministic parameters CFR and TFRAGLIMT: optimistic and

pessimistic; and three containment fragility limits: 25 kPa·s (hatch-door), 50 kPa·s (reinforced hatch-door) and 80 kPa·s (containment base). Results are provided given 99.9% confidence level and 0.001 screening frequency.

According to the results, failure of the containment basemat is expected only in case of large Ø300 mm jet releases and conservative combination of the deterministic parameters (see **Figure 7**a). The failure domain has a non-trivial dependence with respect to the water pool depth. Apparently, deep water pools tend to keep the epicenter of the explosion impulse away from the basemat, in such way decreasing actual loads. Similar, shallow water pools also tend to demonstrate week explosion, behavior probably resulting from decreased level of explosion confinement. Interestingly, failure of the containment basemat is not imminent: **Figure 7**b demonstrates that the failure domain practically disappears at the screening frequency of 0.5, i.e. in 50% of all outcomes the containment basemat will not be damaged with 99.9% confidence level even assuming pessimistic distributions for deterministic parameters.


| a | b |
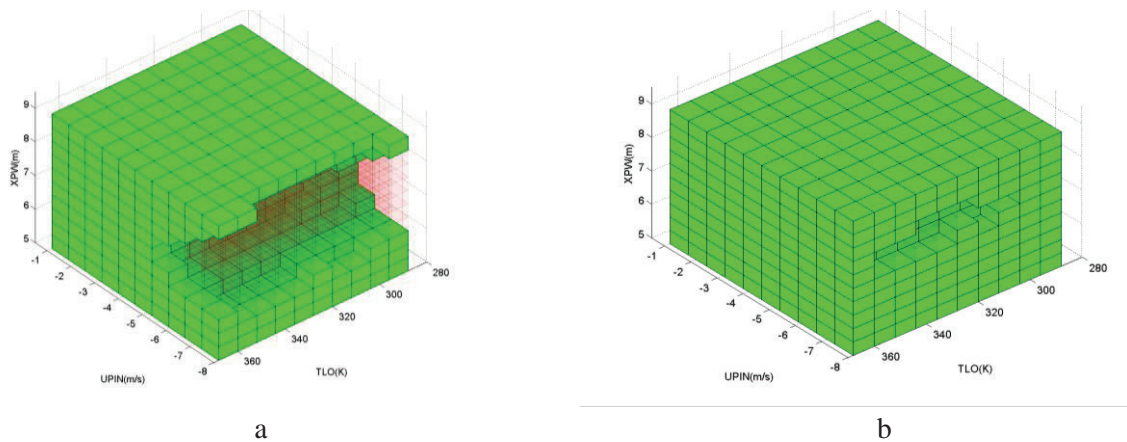
Figure 7: Failure domain for the containment basemat (80 kPa·s) given Ø300 jet (pessimistic assumptions)
a – screening threshold 0.001; b – screening threshold 0.5

If impulses in the location of the hatch door were the same as at the basemat center then the following could be considered. Failure of the reinforced hatch door is predicted possible in the case of intermediate jet diameters (Ø150 mm). However, results in **Figure 8** suggest that improved knowledge on the actual distribution of the deterministic parameters could help to resolve the associated risk.

| a | b |
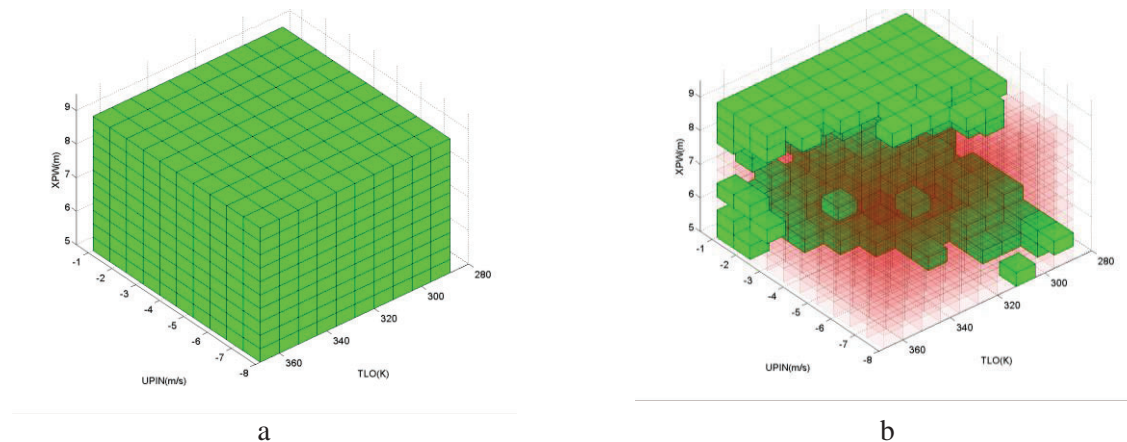
Figure 8: Failure domain for the reinforced hatch door (50 kPa·s) given Ø150 mm jet
a – optimistic; b – pessimistic

The non-reinforced hatch door is subject to failure in most of the accident scenarios even considering optimistic assumptions, i.e. improved knowledge is not likely to resolve the issue of non-reinforced hatch door failure and improvement of the mitigation strategy is required.

a   b
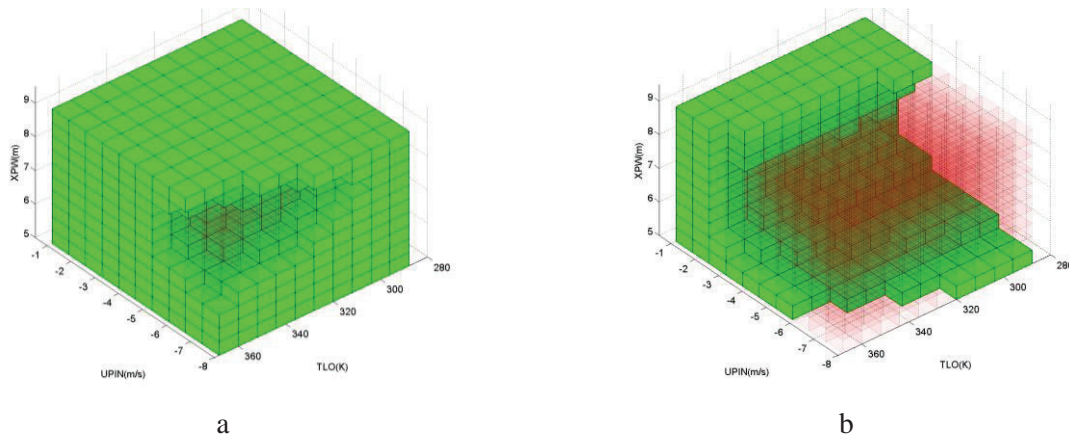
Figure 9: Failure domain for the non-reinforced hatch door (20 kPa·s) (optimistic assumptions)
a – Ø070 mm jet; b – Ø150 mm jet

We must stress that results provided here are of a preliminary nature, the failure domains are dependent on the implemented model for impulse propagation and maturity of the SM.

4.   CONCLUSIONS

In this article we have suggested a robust methodology for the analysis of the steam explosion impact on the Nordic BWR using the 1 dimensional TEXAS-V code. We have demonstrated how TEXAS-V can be used to construct a model of the Nordic BWR in conjunction with a simplified approach to propagate explosion impulses.

Simulations have revealed that explosion impulse is a chaotic function of the triggering time – phenomena that has important impact on both risk analysis and interpretation of experimental results. Specifically, it was demonstrated that explosion impulse can change 50 times within just a 110 ms time window. In integral explosion tests, aleatory uncertainty in the triggering time and melt release conditions is expected to outweigh integral effects of intentionally varied experimental parameters.

We have further, suggested an approach to encompass the chaotic nature of the explosion impulse by characterizing its statistical distribution. The objective is double fold, first it imposes well-posedness on the response function and second allows characterization of the explosion impulse in terms of confidence intervals and confidence levels – approach relevant for risk assessment.

In the second part we have used reverse analysis for identification of the failure domain of a Nordic BWR due to steam explosion. High numerical costs of the analysis required development of a surrogate model of TEXAS-V. The model was implemented using ANNs, validated and integrated into the framework for the reverse analysis. We emphasized on the application of the results for the analysis of the mitigation strategy. Specifically, we demonstrate how knowledge of the failure domain can be used to identify necessary points of improvement in the modelling and necessary modifications in the mitigation strategy.

Quantitative results provided here are still subject to change due to yet immature nature of the implemented SM and assumptions. The principle approach, however, is expected to stay unchanged.

REFERENCES

1. Chu, C.C., One dimensional transient fluid model for fuel-coolant interaction. 1986, university of Wisconsin-Madison.
2. Kim, B.J., Heat transfer and fluid flow aspect of small-scale single droplet fuel-coolant interaction. 1985, University of Wisconsin-Madison.
3. Tang, J., MODELING OF THE COMPLETE PROCESS OF ONE-DIMENSIONAL VAPOR EXPLOSIONS. 1993, University of Wisconsin-Madison.
4. Corradini, M.L., et al., Users' manual for Texas-V: One dimensional transient fluid model for fuel-coolant interaction analysis. 2002, University of Wisconsin-Madison: Madison WI 53706.
5. Murphy, J., A Hydrogen Generation Model for TEXAS. 1992, University of Wisconsin.
6. Park, I.K., D.H. Kim, and J.H. Song, Steam explosion module development for the MELCOR code using TEXAS-V. Journal of Korean Nuclear Society, 2003. 32(4): p. 286-298.
7. Song, J.H., I.K. Park, and J.H. Kim, A coherent methodology for evalluation of a steam explosion load using TEXAS-V. Journal of Korean Nuclear Society, 2004. 36(6): p. 571-581.
8. Chen, R.H., et al., Analysis of KROTOS Steam Explosion Experiments Using the Improved Fuel-Coolant–Interaction Code TEXAS-VI. Nuclear Science and Engineering, 2013. 174: p. 46-59.
9. P. Kudinov et al., "A Framework for the Assessment Of Severe Accident Management Effectiveness in Nordic BWR", Proceedings of PSAM 12, June 2014, Honolulu, Hawaii
10. Theofanous, T.G., On the proper formulation of safety goals and assessment of safety margins for rare and high-consequence hazards. Releability engineering and system safety, 1996. 54: p. 243-257.
11. Theofanous, T.G. and T.-N. Dinh, Integration of multiphase science and technology with risk management in nuclear power reactors. Multiphase Sciense and Technology, 2008. 20(2): p. 81-211.
12. Kudinov, P. and M.V. Davydov. Development of Surrogate Model for Prediction of Corium Debris Agglomeration. in ICAPP-2014. 2014. Charlotte, USA.
13. Hamby, D.M., A review of techniques for parameter sensitivity analysis of environmental models. Environmental Monitoring and Assessment, 1994. 32: p. 135-154.
14. Saltelli, A., et al., Sensitivity analysis in practice: a guide to assessing scientific models. 2004: John Wiley & Sons Inc. 219.
15. Damiani, C., et al., Parameter sensitivity analysis of stochastic models: Application to catalytic reaction networks. Computational Biology and Chemistry, 2013. 42(0): p. 5-17.
16. Corradini, M.L., et al., Fuel-Coolant interaction analysis with TEXAS-V vapor explosion model. 1999: University of Wisconsin.